# The Ouroborand: A Cavitand with a Coordination-Driven Switching Device**

*Fabien Durola and Julius Rebek, Jr.**

Molecular devices reproduce on the nanoscale functions of macroscopic objects, at least notionally:[1] self-assembled capsules are reaction flasks;[2] catenanes and rotaxanes are machines;[3] cylindrical molecular containers can be spring-loaded;[4] and any number of biaryl nanomachines behave as rotors.[5] On/off switches involving extension/contraction motions[6] are among the oldest[7] molecular devices and here we revisit the conformational changes offered by bipyridine rotors to regulate access to a deep cavitand.

Intermolecular forces and the appropriate filling of space usually control the binding of guests inside cavitands. Consider the resorcinarene-based deep cavitand (host) whose fourth wall is functionalized[8] with a bipyridyl switching device linked to a cyclohexyl group (guest). With a flexible linker of appropriate length, this intramolecular guest will reach and occupy the cavity's space. The entropic advantage of the tethered cyclohexane is expected prevent entry of external guests (Scheme 1).

Since such a structure allows this compound to include itself, the name "ouroborand" seemed appropriate to us: Ouroboros ("tail-eater" in Greek) is an ancient symbol representing a serpent swallowing its own tail. It often represents eternity and cycles, but was also frequently used in alchemical illustrations. It inspired Kekule's formulation of benzene and in the more recent chemical literature, Ouroboros was used to describe self-threading molecules.[9] For the case at hand, the favored conformation of the free bipyridine is, as usual, *anti*. This conformation allows the guest fragment (cyclohexyl) to access the cavity in an intramolecular sense and prevents another guest from entering (Scheme 2, config. **A**). When a suitable metal ion is present the bipyridine ligand adopts the chelating *syn* structure. This forces a conformational change that pulls the guest out the cavity (config. **B**), leaving it accessible to an external guest, an adamantane derivative (config. **C**). On removal of the metal ion (config. **D**), the initial configuration is regenerated when the adamantane is released.
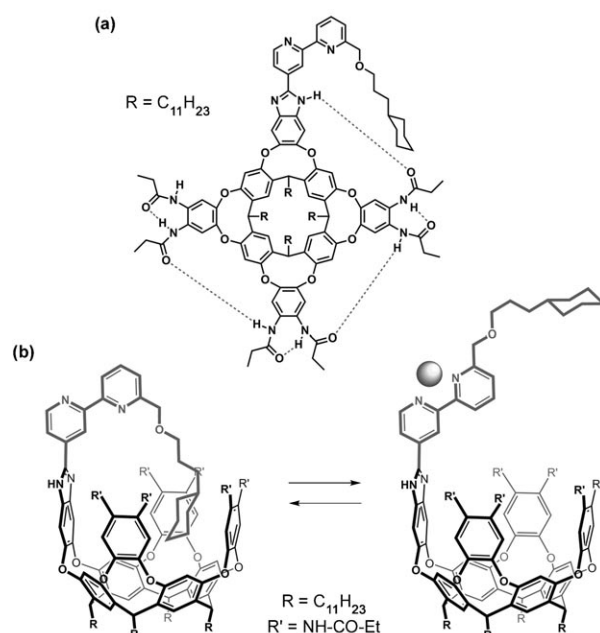
Scheme 1. Representations of the ouroborand; a) planar formula and b) perspective views with the bipyridine ligand free or chelating a metal center.
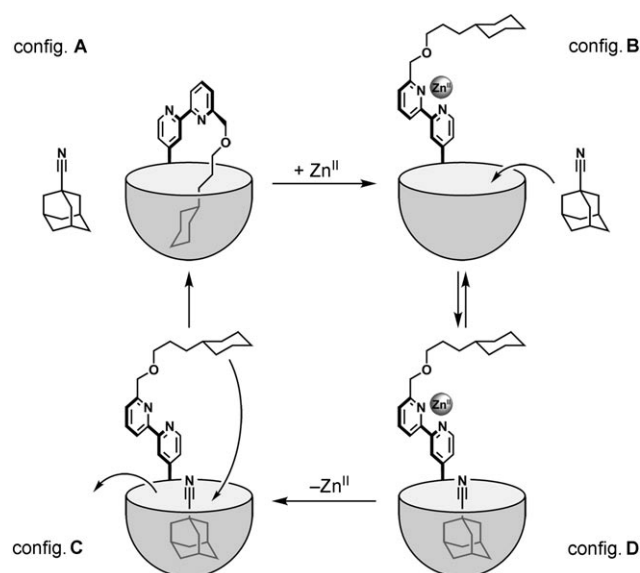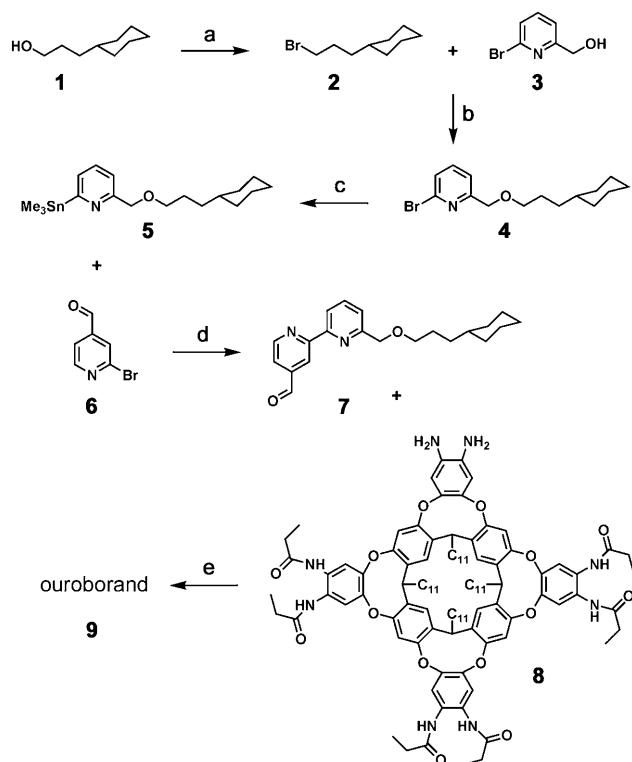

Scheme 2. Reversible mechanism of the coordination controlled guest exchange in the ouroborand's cavity.

[*] Dr. F. Durola, Prof. Dr. J. Rebek, Jr.
The Skaggs Institute for Chemical Biology and Department of Chemistry, The Scripps Research Institute
10550 N. Torrey Pines Road, La Jolla, CA 92037 (USA)
Fax: (+1) 858-784-2876
E-mail: jrebek@scripps.edu
Homepage: http://www.scripps.edu/skaggs/rebek/

The ouroborand was synthesized in ten steps from commercially available compounds (Scheme 3) and was characterized by ^{1}H NMR and mass spectrometry.[10] Diamino

Scheme 3. Synthesis of the ouroborand. a) PBr₃, 0°C 15 min, RT 2 h, 100°C 1.5 h, 100%; b) NaH, THF, RT 2 h, 75°C 16 h, 26%; c) BuLi, toluene, −20°C, −78°C 2 h, Me₃SnCl, −78°C 1 h, RT, 55%; d) [Pd-(PPh₃)₄], toluene, 110°C 48 h, 75%; e) dioxane, RT 30 min, 100°C 16 h, 67%.

cavitand **8** was obtained in five steps by following an efficient and well-established procedure.[8] Primary alcohol **1** was first brominated by using phosphorus tribromide, then the corresponding bromoalkane **2** was used with alcohol **3** in a Williamson reaction, with sodium hydride as a base to give the ether **4**. The yield of that last step was modest due to the multiple reactivity of (6-bromopyridin-2-yl)methanol (**3**), but fortunately the reaction can be done on a large scale. The bromopyridine **4** was then converted to the stannylpyridine **5** by forming first an organolithium compound with *n*-butyl-lithium, and then by reaction with trimethyltin chloride under classical conditions. The tin compound **5** so obtained was then reacted with another bromopyridine **6**, following Stille cross-coupling conditions with [Pd(PPh₃)₄] as a catalyst, to give the bipyridine **7** in a typical yield. The aldehyde function of the bipyridine-incorporating tether was ultimately attached to the diamino cavitand **8**, by formation of an imidazole aromatic ring, to give the ouroborand **9**.

The autophagic behavior of this molecule could be established in different deuterated solvents by ¹H NMR. Because the cavitand's walls incorporate eight aromatic rings, any guest molecules in the cavity are exposed to a strong shielding effect, which shifts the ¹H NMR signals upfield, below $\delta = 0$ ppm. [D₁₂]Mesitylene (1,3,5-trimethylbenzene) is a common NMR solvent for the study of cavitands. Although its concentration is ca. 10 M, its shape is not accommodated and it does not compete with other molecules for access to the

cavity. Integration of the upfield NMR signals in this solvent reveals that all cyclohexyl hydrogen atoms of the ouroborand and even a part of the linker chain are located in the cavity, (see Figure 2a). Another telltale feature of the spectrum is the AB pattern of signals corresponding to the pyridine-*CH₂*-O protons. They are diastereotopic and appear as two well-separated doublets, located between 4 and 5 ppm, with a large coupling constant ($^2J = 13$ Hz) (Figure 1a). Such a difference
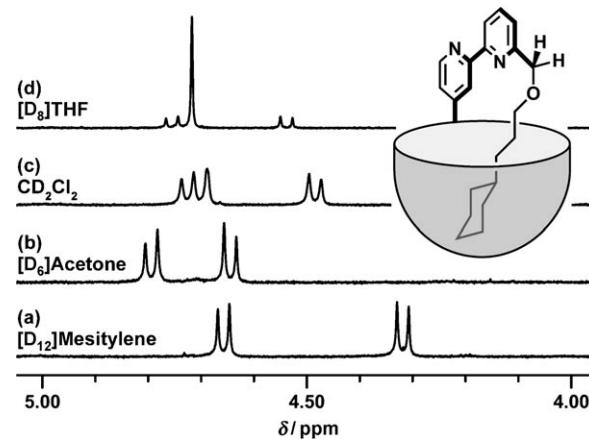

Figure 1. NMR signals of the pyridine-*CH₂*-O protons when the ouroborand is solubilized in deuterated a) mesitylene, b) acetone, c) dichloromethane, or d) THF. Doublets correspond to the cartoon shown whereas singlets correspond to solvent-occupied cavitands.

between these seemingly identical protons arises from the asymmetry of the environment: the head-to-tail arrangement of the secondary amides on the rim the cavitand is directional and set by the chain of hydrogen bonds that terminate at the benzimidazole. The arrangement may be as shown in Scheme 1 or, through tautomerization of the benzimidazole, its mirror image and the interconversion of these cyclo-enantiomers is slow on the NMR timescale of the experiments. Dimeric or oligomeric assemblies of the ouroborand are excluded by the simplicity of the spectra. Similar results are observed in [D₆]acetone (Figure 1b), despite the smaller size of the solvent. In [D₂]dichloromethane (Figure 1c), the solvent molecule (at a concentration of ca. 10 M) is a good guest and competes for the cavitand. Some cyclohexyl groups are regurgitated from the cavity, and a broadened singlet appears for the pyridine-*CH₂*-O protons, which are now at some distance from the asymmetric environment. In [D₈]THF (Figure 1d), a solvent that is a very good guest (and again, is present in multimolar concentration) most of the cavitands contain THF molecules, but almost 20% still cling to the cyclohexyl "tail", a testimony to the advantages of the intramolecular interaction.

Some experimentation was required to optimize the reversible switching process in this system. The primary solvent was [D₁₂]mesitylene but 20% [D₃]acetonitrile (a somewhat poor guest for the cavitand) was required to dissolve the metal complexes. Dilute solutions (1 mM, 2 mg mL⁻¹) precluded intermolecular interaction between cavitands. An excess of the free guest, 1-adamantane-carbo-nitrile (AdCN), which is typically an excellent neutral guest for cavitands,[11] and an excess of ZnBr₂ as the metal source

were used. These excesses were necessary to drive the coordination and represented the best conditions for observation of reversible switching between the two states.

Figure 2 shows the evolution of the ^{1}H NMR spectra during the steps of the switching cycle. The changes appeared mainly in two parts of the spectrum: Between $\delta = 3$ and 5 ppm, signals integrate for the four pyridine-*CH$_2$-O-CH$_2$*-protons; below $\delta = 0$ ppm, signals only correspond to protons located in the cavity. The use of [D$_3$]acetonitrile slightly broadens the signals but does not interfere with the self-hosting of the cyclohexyl group (Figure 2 a). Addition of 10 equivalents of AdCN to the NMR solution (Figure 2 b) causes no changes; the cavitand is inaccessible to this external guest. But on addition of 10 equivalents of ZnBr$_2$ (Figure 2 c), the doublets between $\delta = 5$ and 3 ppm are converted to singlets, showing that the coordination-induced switching of the system is complete. The flexible tail is now outside the cavity and the chirality of the system is too remote to affect the geminal CH$_2$ coupling. Integration of the signals below $\delta = 0$ ppm shows that only 45 % of the cavitand is occupied with AdCN molecules. The remaining cavitand is presumably solvent-filled because the AdCN occupancy decreases when more than 20 % of [D$_3$]acetonitrile or less than 10 equivalents of AdCN is used. Accordingly, two different singlets appear around $\delta = 4.6$ ppm, integrating for the -pyridine-*CH$_2$*-O-protons, with a 55:45 ratio. The Zn^{II} complex is labile but can be observed by mass spectrometry (MALDI) as [Zn(ouroborand)Br]$^+$. Since a bis(ouroborand) complex would be more stable, this result implies that the zinc(II) cation is coordinated to only one ouroborand. After addition of water to the NMR sample, followed by separation of the organic phase and drying over Na$_2$SO$_4$, the spectrum is very similar to the one after addition of AdCN to the ouroborand (Figure 2 d). The zinc ions were extracted into the aqueous phase, and allowed the system to revert to the self-hosting state with the concomitant release of the AdCN molecules to the bulk solution.
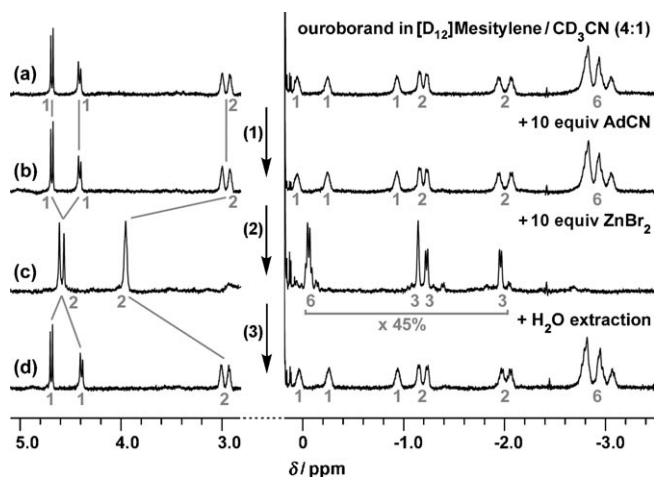
Some dynamic molecular capsules that can change cavity sizes have been developed[12] but only few examples of systems combining molecular machines[13] and supramolecular chemistry[14] have been reported in the literature. Here, we used a bipyridyl rotor in an intramolecular setting to open or close access to guests through metal coordination-driven switching. To place these results in an historical perspective, we note that bipyridyl rotors[15] were among the earliest chemical models of allosteric behavior of proteins—how binding at a remote site can alter the behavior of an active site.[16] More recently, bipyridyls attached to cavitands were introduced by Lützen[17] to control chelation of guests. The most recent applications, involving metal chelation that results in changes resembling flapping motions[18] indicate that the predictable consequences of bipyridyl/metal chelation are reliable tools for forging tomorrow's molecular machinery.

[1] V. Balzani, A. Credi, M. Venturi in *Molecular Devices and Machines*, Wiley-VCH, Weinheim, **2003**, chap. 12.

[2] M. Yoshizawa, J. K. Klosterman, M. Fujita, *Angew. Chem.* **2009**, *121*, 3470–3490; *Angew. Chem. Int. Ed.* **2009**, *48*, 3418–3438.

[3] a) V. Balzani, A. Credi, F. M. Raymo, J. F. Stoddart, *Angew. Chem.* **2000**, *112*, 3484–3530; *Angew. Chem. Int. Ed.* **2000**, *39*, 3348–3391; b) S. Bonnet, J.-P. Collin, M. Koizumi, P. Mobian, J.-P. Sauvage, *Adv. Mater.* **2006**, *18*, 1239–1250.

[4] D. Ajami, J. Rebek, Jr., *J. Am. Chem. Soc.* **2006**, *128*, 15038–15039.

[5] E. R. Kay, D. A. Leigh, F. Zerbetto, *Angew. Chem.* **2007**, *119*, 72–196; *Angew. Chem. Int. Ed.* **2007**, *46*, 72–191.

[6] M.-C. Jiménez, C. Dietrich-Buchecker, J.-P. Sauvage, *Angew. Chem.* **2000**, *112*, 3422; *Angew. Chem. Int. Ed.* **2000**, *39*, 3284.

[7] S. Shinkai, T. Nakaji, Y. Nishida, T. Ogawa, O. Manabe, *J. Am. Chem. Soc.* **1980**, *102*, 5860–5865.

[8] A. R. Renslo, J. Rebek, Jr., *Angew. Chem.* **2000**, *112*, 3419–3421; *Angew. Chem. Int. Ed.* **2000**, *39*, 3281–3283.

[9] S. Nygaard, Y. Liu, P. C. Stein, A. H. Flood, J. O. Jeppesen, *Adv. Funct. Mater.* **2007**, *17*, 751–762.

[10] See Supporting Information for details.

[11] R. J. Hooley, S. R. Shenoy, J. Rebek, Jr., *Org. Lett.* **2008**, *10*, 5397–5400.

[12] D. Ajami, J. Rebek, Jr., *Nat. Chem.* **2009**, *1*, 87–90.

[13] Special issue: a) *Acc. Chem. Res.* **2001**, *34*, 409–522; b) J.-P. Sauvage, *Struct. Bonding (Berlin)* **2001**, *99*.

[14] a) M. Barboiu, J.-M. Lehn, *Proc. Natl. Acad. Sci. USA* **2002**, *99*, 5201–5206; b) A. Petitjean, R. G. Khoury, N. Kyritsakas, J.-M. Lehn, *J. Am. Chem. Soc.* **2004**, *126*, 6637–6647.

[15] J. Rebek, Jr., J. E. Trend, *J. Am. Chem. Soc.* **1978**, *100*, 4315–4317.

[16] J. Rebek, Jr., J. E. Trend, R. V. Wattley, S. Chakravorti, *J. Am. Chem. Soc.* **1979**, *101*, 4333–4337.

[17] a) A. Lützen, O. Haß, T. Bruhn, *Tetrahedron Lett.* **2002**, *43*, 1807–1811; b) S. Zahn, W. Reckien, B. Kirchner, H. Staats, J. Matthey, A. Lützen, *Chem. Eur. J.* **2009**, *15*, 2572–2580.

[18] S. Ulrich, J.-M. Lehn, *J. Am. Chem. Soc.* **2009**, *131*, 5546–5559.

Figure 2. NMR study of the coordination-triggered switch and guest exchange of the ouroborand; 1) 10 equivalents AdCN added in the NMR tube; 2) 10 equivalents ZnBr$_2$ added in the NMR tube; 3) water added to the NMR tube, then extraction and drying on Na$_2$SO$_4$. Integration values are shown in gray.